Eur. Phys. J. D **35**, 207–216 (2005)
DOI: 10.1140/epjd/e2005-00078-8

THE EUROPEAN PHYSICAL JOURNAL D

Electronic interaction between valence and dipole-bound states of the cyanoacetylene anion

T. Sommerfeld[1,a] and S. Knecht[2]

[1] University of Pittsburgh, Department of Chemistry, Chevron Science Center, 219 Parkman Avenue, Pittsburgh PA 15260, USA
[2] Universität Heidelberg, Physikalisch-Chemisches Institut, Im Neuenheimer Feld 229, 69120 Heidelberg, Germany

Received 23 March 2005 / Received in final form 23 April 2005
Published online 7 June 2005 – © EDP Sciences, Società Italiana di Fisica, Springer-Verlag 2005

Abstract. The electron attachment properties of cyanoacetylene HCCCN are investigated with particular emphasis on the coupling between dipole-bound and valence states. As an initial step both the dipole-bound and the valence state of $HCCCN^-$ are studied separately using high level ab initio methods. Predictions for the geometry of the valence anion, the electron binding energy of the dipole-bound state, the energy of the temporary anion associated with vertical attachment into the valence state, the vertical detachment energy of the valence anion, and the adiabatic electron affinity of HCCCN are given. Our results indicate that the electron affinity found in the NIST web-book is not that of HCCCN but of some other C_3HN species. The two anionic states interact with each other, and we study their electronic coupling by computing the two electron binding energies along one- and two-dimensional cuts through the potential energy surfaces, and fitting a diabatic model potential to the ab initio data. In particular, the two-dimensional cuts allow us to examine the geometry dependence of the electronic coupling, and to ask the question whether the coupling elements inferred from one-dimensional cuts represent typical values. Moreover, the influence of the theoretical method on the computed coupling elements is investigated, and the possibility of employing the diabatic model potential as a mean to extrapolate bound state binding energies into the metastable domain is pointed out.

PACS. 31.50.Gh Surface crossings, non-adiabatic couplings – 31.50.Bc Potential energy surfaces for ground electronic states – 34.70.+e Charge transfer – 34.80.Gs Molecular excitation and ionization by electron impact

1 Introduction

Cyanoacetylene HCCCN is a linear molecule and belongs to the group of 125+ molecules that have so far been detected in interstellar or circumstellar space (see e.g. web-page of the National Radio Astronomy Observatory `www.cv.nrao.edu`). Owing to its large dipole moment of 3.72 Debye [1], HCCCN will readily attach an 'excess' electron in a dipole-bound state [2–4], and since its unsaturated π–system virtually guarantees the existence of a low-lying valence anion state, the HCCCN molecule is an ideal candidate to study the interaction between these two fundamentally different anion types.

Before discussing the electronic coupling between valence and dipole-bound states let us briefly introduce these two anion classes. Valence or conventional anions are formed when an excess electron is put into an unoccupied valence orbital of a neutral molecule. These orbitals are typically anti-bonding in character, say σ^* or π^*, and therefore electron attachment will lead to some geometrical distortion, and the equilibrium structure of a valence anion is in most cases markedly different from that of the neutral system. On the other hand, an electron can be bound exclusively by long-range potentials such as the dipole potential of a neutral molecule (for reviews see [2–4] and several articles in [5]). Dipole-bound states are typically very diffuse with most of the excess electron's density residing outside the van-der-Waals-surface of the neutral, and consequently, dipole-bound electrons have little influence on the geometrical structure. Let us note that there is no sharp distinction between dipole-bound and more conventionally bound species. For example, $NaCl^-$ is a borderline case that can be understood as a dipole-bound or as a valence (attachment into a Na $3s/3p$ hybrid orbital) anion.

In any molecular system displaying both conventional and dipole-bound anion states these states will interact. This interaction is associated with intramolecular electron transfer from the molecular periphery onto the nuclear framework (or vice versa), and it has been invoked as key

[a] e-mail: `thomas@theory.chem.pitt.edu`

step in processes such as Rydberg electron transfer [6,7], free electron attachment to clusters [8–10], and electron-induced bond-cleavage [11–13]. Nevertheless, only very little is known about the details of the electronic interaction. So far there are rough estimates for the coupling of only three molecules: nitromethane, uracil, and 5-chlorouracil, and for all three systems coupling elements in the order of several 10 meV have been found [14–16].

In the previous studies [14–16] the coupling estimates have been inferred from ab initio calculations by computing one-dimensional cuts through the relevant potential energy surfaces, and fitting an avoided crossing model potential to the ab initio data. In this paper our main goal is to go beyond the one-dimensional treatment and to investigate the electronic coupling in more dimensions. In particular we aim at answering the questions over what range the coupling varies in the relevant regions of nuclear coordinate space, and whether a one-dimensional treatment will yield a typical value. Second, we will examine the influence of the theoretical method employed to compute the potential surfaces. Specifically, we shall compare an highly efficient second order electron propagator method with a more accurate though more demanding equation-of-motion coupled-cluster scheme. HCCCN was chosen for this purpose, since the geometrical changes induced by adding an electron to its lowest unoccupied valence orbital affect — to a good approximation — only two coordinates: the HC–CCN bond length and one bending coordinate. This allows us to restrict our attention to a two-dimensional potential energy surface. In addition, HCCCN is a relative small molecule, and we could afford high-level ab initio calculations at more than 600 grid points.

At the same time this is a study of the electron attachment properties of HCCCN. To our best knowledge, neither the geometrical structure of the $HCCCN^-$ valence anion nor the electron binding energies associated with the two anion states have been reported so far. We computed the geometrical structure of the valence anion, and we will give high level ab initio values for four key observables: (1) the vertical electron affinity (EA) of the dipole bound state, (2) the resonance energy associated with vertical attachment to the lowest π^* valence orbital, (3) the vertical detachment energy of the valence state, and (4) the adiabatic EA of the valence state. Based on our results, we will in particular argue that the adiabatic EA found in the NIST database is not that of cyanoacetylene but that of a different, so far unidentified C_3HN species. The paper is organized as follows. In the next section we outline the ab initio methods that have been employed to compute positive and negative electron binding energies of cyanoacetylene. Then, as a first step, the vertical and adiabatic EAs of HCCCN are studied in Section 3. The main part of the paper is Section 4 where the dipole-valence coupling is studied by means of model potentials fitted to one and two-dimensional cuts through the potential energy surfaces of the two lowest anionic states. Our conclusions are summarized in Section 5.

2 Ab initio methods

The electron binding energy (EBE) of HCCCN has been computed using two principle approaches. On the one hand, the total energies of neutral and anion were calculated at the following ab initio levels of theory: self consistent field (SCF), second order Møller-Plesset perturbation theory (MP2), coupled cluster with single and double substitutions (CCSD), and CCSD with non-iterative triple substitutions (CCSD(T)). The difference of the total energies is the EBE, and we refer to these values as ΔSCF, ΔMP2, ΔCCSD, and ΔCCSD(T). On the other hand, the EBE can be obtained *directly* using electron propagator or response theory based approaches (see e.g. [17,18]). We have employed the second order Green's function (ADC(2)) [19] and the equation-of-motion coupled-cluster (EOM-CCSD) [20] methods. The relations between these and other direct approaches can advantageously be understood in the framework of intermediate state representations [21,22], and these articles contain many references to earlier work in this large field. One can understand the direct methods as higher order corrections to the energy of an unoccupied HF orbital that represents the zeroth order approximation for the EBE (Koopmans' Theorem (KT)). In this many-body perturbation theory sense ADC(2) is a second order and EOM-CCSD is a third order scheme. Both direct and indirect methods have certain advantages and disadvantages. If only a single state (the ground state) is considered indirect methods yield — at comparable computational cost — typically more accurate values. However, if more than one state is needed, or if two states are close in energy, direct methods are called for.

All methods described so far always imply that the considered anionic states are stable with respect to vertical autodetachment. This is, however, not the case at the equilibrium geometry of neutral HCCCN, where the valence state is unstable with respect to electron autodetachment. To compute the associated temporary or resonance state we used the complex absorbing potential method (CAP) [23,24] at the frozen orbital and at the ADC(2) levels of theory [25,26]. Loosely speaking, a CAP is added to the Hamiltonian to absorb the outgoing electron, and in this way the sought resonance state can be described with a square-integrable wavefunction. In a CAP calculation one obtains the complex Siegert energy $E_r - i\Gamma/2$ of the temporary state, where E_r is the resonance position ($-E_r$ is the negative EA) and the width Γ is the inverse of the autodetachment lifetime $\tau = \hbar/\Gamma$.

In all bound state calculations the augmented correlation-consistent polarized valence double-ζ (AUG-cc-pVDZ) and triple-ζ (AUG-cc-pVTZ) basis sets [27] were used. These two sets were further augmented by a diffuse 8s8p set centered on the H atom (even tempered exponents starting from the standard diffuse exponents; scaling factor 3.5) whenever the dipole-bound state was considered. In the CAP calculations for the the π^* resonances we employed a valence triple-ζ set [28] augmented with a 9p set of diffuse functions (TZVP+9p) centered on all non-hydrogen atoms (even-tempered exponents starting

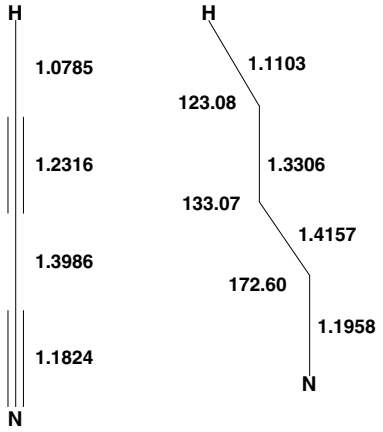

Fig. 1. Schematic structures of neutral HC_3N and its valence anion. The bond length and angles have been obtained at the CCSD(T)/AUG-cc-pVDZ level of theory. Lengths (in Å) are given on the right hand side and angles (in degrees) on the left hand side of the structures.

from the smallest p-exponent in the valence set; scaling factor 1.8).

All MP2 and coupled-cluster calculations were carried out with the Aces II code [29]. For ADC(2) and CAP/ADC(2) calculations our own codes were used, which build on the transformed integrals produced by the MOLCAS5 package [30].

3 Electron affinity

In this section we consider vertical and adiabatic electron attachment to HCCCN. This sets the stage for studying the interaction between the dipole-bound and the valence states, and yields predictions for the four observables: Adiabatic EA, vertical detachment energy (VDE) of the anion, electron affinity associated with the dipole-bound state EA_{DB}, and the resonance position E_r of the temporary π^* state. The first step in these calculations is to establish the equilibrium structures of neutral and anion. The structure of the neutral is known [1], but that of the anion is not. To be consistent we performed geometry optimizations and frequency calculation for both neutral and anion at the CCSD(T)/AUG-cc-pVDZ level of theory, and these geometries where used in all subsequent calculations. The results are shown in Figure 1. Neutral HCCCN is a linear closed-shell molecule with a $^1\Sigma^+$ electronic ground state, and the computed bond lengths are in fair agreement with the experimental data [1]. The valence anion shows a trans-bent zig-zag structure (C_s symmetry, $\angle(\mathrm{HCC}) = 123°$, $\angle(\mathrm{CCC}) = 133°$.) and an $^2\mathrm{A}'$ electronic ground state. Note that upon electron attachment only one of the bond lengths changes strongly: the CC triple bond of the neutral is stretched by about 0.1 Å. We did not find any cis-bent minimum.

Table 1. Electron binding energy of the dipole-bound state. The results have been obtained at the CCSD(T)/AUG-cc-pVDZ geometry of the neutral. Zero-point effects are not included. All values in meV.

	AUG-cc-pVDZ+8s8p	AUG-cc-pVTZ+8s8p
ΔSCF	5.8	5.8
ΔMP2	7.1	7.5
ΔCCSD	8.4	9.4
ΔCCSD(T)	7.7	8.7
KT	5.1	5.1
ADC(2)	22.3	—
EOM-CCSD	13.4	14.2

3.1 Dipole-bound state

At the geometry of the neutral the only bound state of the cyanoacetylene anion is the $^2\Sigma^+$ dipole-bound state. Its EBE computed at different levels of theory is collected in Table 1. Since the computed values are more than two orders of magnitude larger than the rotational constants of HCCCN, the influence of the rotation of the molecular framework on the binding energy should be negligible [31]. From the results at increasingly sophisticated levels of theory one can conclude [2,32] that electrostatic interactions, polarization, and electron correlation effects contribute roughly 59, 7, and 34 % to the binding energy. Thus, despite the very diffuse orbital of the dipole-bound electron, electron correlation effects are absolutely crucial to describe the binding, making cyanoacetylene a typical member of this anion class. Comparing the direct methods with the ΔCCSD(T) result, which is presumably our most reliable value, we find that at the second order ADC(2) level the EBE is over-corrected from its too small 0th order value. In contrast, the third order EOM-CCSD result is reasonably close to the ΔCCSD(T) value similar to what was found for other dipole-bound anions (see e.g. [33]). Regarding the underlying one-particle basis set, let us mention that it is well known that flexible valence basis sets are needed for dipole-bound species [34], and in going from the double-ζ to the triple-ζ basis set — at all correlated levels of theory — the computed binding energy notably increases. Neglecting geometrical relaxation and zero-point motion effects, which are expected to be small, based on the CCSD(T) value we predict cyanoacetylene to posses a dipole-bound anion with an EBE of about 9 meV.

3.2 Resonances

The cyanoacetylene molecule has two unoccupied π^* orbitals, and putting an additional electron into one of these orbitals leads to temporary anion states that lie in the neutral-plus-free-electron continuum. Using our CAP methods we have computed the Siegert energies of these two $^2\Pi$ resonance states at the frozen orbital (or static-exchange) level and at the ADC(2) level where polarization and electron correlation effects are included within second order perturbation theory. In a CAP calculation one needs to identify the sought resonances among the

Table 2. Resonance positions and widths of the two $^2\Pi$ resonances of $HCCCN^-$. The TZVP+9p basis set has been used. All values in eV.

	Frozen Orbital		ADC(2)	
	E_r	Γ	E_r	Γ
1st resonance	2.1	0.4	0.70	0.15
2nd resonance	9.0	2.5	6.2	1.1

Table 3. Vertical detachment energy of $HCCCN^-$. The geometry has been optimized at the CCSD(T)/AUG-cc-pVDZ level, and the values are given in eV.

	AUG-cc-pVDZ	AUG-cc-pVTZ
ΔSCF	1.54	1.55
ΔMP2	0.92	1.03
ΔCCSD	1.21	1.35
ΔCCSD(T)	1.10	1.25
KT	0.46	0.46
EOM-CCSD	1.14	1.26

many discretize continuum states, and one needs to optimize the strength η of the absorbing potential [24]. These two issues are in fact closely related since the so-called η-trajectories of the resonances stabilize at the optimal η, and the stabilization as such is one of the criteria used to identify the resonances. In our calculations with the TZVP+9p basis set it is straightforward to identify the two resonance states and to find the optimal η values. Our results are collected in Table 2. Both states are short-lived shape-type resonances, and as usual, the inclusion of polarization and electron correlation 'stabilizes' the resonances in the sense that lower positions and smaller widths are found. For HCCCN we did not find any experimental data to compare with, but for other shape-type resonances it has been found that the ADC(2) results obtained with basis sets of TZVP quality provide good approximations (typically a few tenths of an eV too high) for the resonance positions measured by electron transmission spectrometry [26].

3.3 Adiabatic EA

Before considering the adiabatic EA, it is important to establish that the valence anion is a bound state at its own equilibrium structure, that is, that its VDE is positive. Our values obtained at different levels of theory are collected in Table 3. The $HCCCN^-$ valence anion is clearly electronically stable at its trans-bent geometry, and apart from the KT result all other values are fairly close to each other. Larger basis sets again slightly 'stabilize' the anion. Our best value is the CCSD(T) result, and we predict a VDE of 1.25 eV. Provided the valence anion can somehow be produced, this prediction can directly be tested in a photo detachment experiment.

Let us now turn to the adiabatic EA. The electronic contribution (uncorrected for zero-point vibrations) obtained at different theoretical levels are listed in Table 4. While the ΔSCF value is clearly negative, all values obtained at correlated levels of theory lie within an interval of ± 0.25 eV suggesting an adiabatic EA close to zero. In particular, at the highest level employed (CCSD(T)/AUG-cc-pVTZ) we find an adiabatic EA of +10 meV, and we conclude that neutral HCCCN and its valence anion are virtually isoenergetic. Thus, the adiabatic EA is essentially determined by the difference in zero-point energies. Already from the structures (Fig. 1) it is clear that this difference cannot be dramatic, and at the CCSD(T)/AUG-cc-pVDZ level we find that the zero-point energy of the anion is 40 meV less than that of the neutral. Thus we predict HCCCN to have an adiabatic EA of 50 meV. We did not find any hints for unusually large correlation effects, and therefore we expect the error in the computed EA to be at most in the 100–200 meV region. Since the computed EA is smaller than its anticipated error bar we performed additional G3 and G3(MP2) calculations [35] that gave adiabatic EAs of 80 and 134 meV respectively. These results are very close to our CCSD(T) value, and we are confident to predict a small ($\lesssim 100$ meV) but positive adiabatic EA for HCCCN.

Table 4. Adiabatic EA of HCCCN. The neutral and anion geometries have been optimized at the CCSD(T)/AUG-cc-pVDZ level. Negative values imply that the anion lies energetically above the neutral. Zero-point effects are not included; all values in eV.

	AUG-cc-pVDZ	AUG-cc-pVTZ
ΔSCF	–0.39	–0.49
ΔMP2	–0.16	–0.23
ΔCCSD	0.01	–0.06
ΔCCSD(T)	0.08	0.01
EOM-CCSD	–0.15	–0.12

Our computed EA is in stark disagreement with the EA found in the NIST web-book: 2.56 ± 0.22 eV. We attribute this discrepancy to the interpretation of the original experimental data. In [36] a "C_3HN^-" species was produced by dissociative electron attachment to cyanoethylene and the associated cross section was reported. However, no structure was assigned to the observed species, and no adiabatic EA was extracted from the cross section. Our calculations definitely rule out that HCCCN possesses an EA in excess of a few 100 meV. Thus, the nature of the observed anionic species will remain an open question, but let us mention that we briefly considered cyanovinylidene which shows a G3(MP2) EA of 1.85 eV much closer to the 2.56 eV from the NIST web-book.

4 Coupling between dipole-bound and valence states

Before discussing the $HCCCN^-$ system, let us briefly review the coupling between valence and dipole-bound anions from a general point of view. There are two ways of thinking about a molecule possessing both a dipole-bound and a valence anion. In an *adiabatic* picture one associates each anion with a different minimum on the lowest adiabatic potential energy surface (PES). Clearly, following

the minimal energy path from the dipole-bound to the valence minimum the character of the electronic wavefunction changes dramatically indicating that the barrier between the two minima is the lower branch of an avoided crossing. Thus, in the adiabatic description the ground and the first excited state are strongly coupled by the nuclear kinetic energy operator, and in the vicinity of the crossing the Born-Oppenheimer approximation breaks down. However, thinking in terms of dipole-bound and valence states does actually imply a diabatic viewpoint. Diabatic states do retain their character when the nuclei move [37,38], and in a diabatic picture the two PES associated with the dipole-bound and the valence state will cross on any path connecting the two respective minima. Clearly, in a diabatic representation the electronic Hamiltonian is — by construction — non-diagonal, and the off-diagonal elements are referred to as the coupling elements or just the coupling. This is in fact the advantage of any diabatic representation; the dominant part of the coupling has been moved from the kinetic energy operator into the electronic Hamiltonian facilitating the description of the nuclear dynamics [37,38].

Just as the adiabatic and diabatic potential energy surfaces, the coupling matrix element is a function of the nuclear coordinates. In our previous investigations we aimed at obtaining a reasonable estimate for the order of magnitude of the coupling element. For nitromethane and uracil we chose a one-dimensional straight line cut connecting the equilibrium structures of the respective dipole-bound and valence anions, computed the adiabatic potential energy curves along the cut, and extracted the coupling by fitting the ab initio results to a simple forbidden crossing model potential [14,15]. Here we investigate the coupling as a function of two coordinates. In this way, we do not only get a typical value, but can study how the coupling varies along the seam of intersection of the two diabatic states where its influence is strongest. Second, we can compare with the coupling obtained in a one-dimensional treatment and in this way check the robustness of our earlier results.

The choice of studying a two-dimensional surface is suggested by the main differences between the neutral and anion geometries (Fig. 1). In going from the neutral structure to that of the valence anion, the CC triple bond is stretched considerably by about 0.1 Å, and the molecule is strongly bent trans (or anti) to the CC triple bond, i.e., the ∠(HCC) and ∠(CCC) angles are decreased by roughly 50°. In contrast the CCN terminus stays essentially linear (bending by 8°), and the other bond lengths change by less than 0.03 Å. Thus, we chose a two-dimensional cut in R and θ, where R is the length of the CC triple bond and θ is the trans bending angle ($\theta = \angle(\mathrm{HCC}) = \angle(\mathrm{CCC})$ with the H–C–C–C dihedral angle being 180°). All other coordinates are held constant; the ∠(CCN) angle is set to 180°, and the three remaining bond lengths are set to the average of their lengths in the neutral and anionic structures. We then reoptimized the two equilibrium geometries subject to the imposed restrictions (only R and θ were varied), and, as expected, the resulting structures and energy differences are in good agreement with those obtained from unrestricted geometry optimizations.

We now turn to the diabatic model potential employed to analyze the ab initio results. In comparison with the model potentials of references [14,15], the ansatz for the diabatic potential has been improved in two respects. In the first place, we included a second dipole-bound state into our diabatic model potential, which now reads

$$\mathbf{V} = \begin{pmatrix} V_1 & W_{12} & W_{13} \\ W_{12} & V_2 & 0 \\ W_{13} & 0 & V_3 \end{pmatrix}, \tag{1}$$

where V_1 is the valence state, V_2 and V_3 represent dipole bound states, and W_{12} and W_{23} are the respective couplings. This step became necessary, since our basis set was sufficiently diffuse to yield a second dipole bound state at least in some regions of nuclear coordinate space. (In the Born-Oppenheimer approximation any molecule having one dipole-bound state has in fact an infinite number thereof — similar to a Rydberg series; due to the finite basis set employed in practical calculations typically only one (or even none) are seen.) The second dipole-bound state has at all geometries an exceedingly small binding energy below 1 meV, and is certainly not converged with respect to basis set size. Yet, it cannot simply be ignored, since in regions where the valence state is a resonance, it represents the second adiabatic state. The extension of the diabatic potential by a third state with zero binding energy (i.e. V_3 is set to be identical with the potential energy surface of the neutral) effectively accounts for the fact that the valence state is actually crossing a series of states, and by this means any traces of additional dipole-bound states in the ab initio data can be accounted for.

In the second place, we took the energy of neutral HCCCN out of the potential

$$\mathbf{V} - V_0\mathbf{1} = \begin{pmatrix} E_1 & W_{12} & W_{13} \\ W_{12} & E_2 & 0 \\ W_{13} & 0 & E_3 \end{pmatrix}, \tag{2}$$

where V_0 is the PES of the neutral, $\mathbf{1}$ is the unit matrix, and E_1, E_2, and E_3 are the EBEs of the valence, first, and second dipole-bound states respectively. In this way we can directly fit the ab initio EBEs obtained at the ADC(2) or EOM-CCSD levels without choosing (or computing) a specific PES for the neutral. A great advantage of this procedure is that the curvature of the EBEs as a function of the nuclear coordinates is typically much smaller than that of the respective PES (cf. e.g. [39]). In other words, while at least quadratic functions of the nuclear coordinates are needed for any reasonable fit of the V_i, for the E_i already linear functions do a good job, and quadratic functions yield excellent fits to the ab initio results (see below).

Having established restricted and unrestricted one-dimensional and a two-dimensional cut through the anionic PES as well as a diabatic model potential, let us now turn to our results. First, we consider the two one-dimensional cuts connecting the respective unrestricted

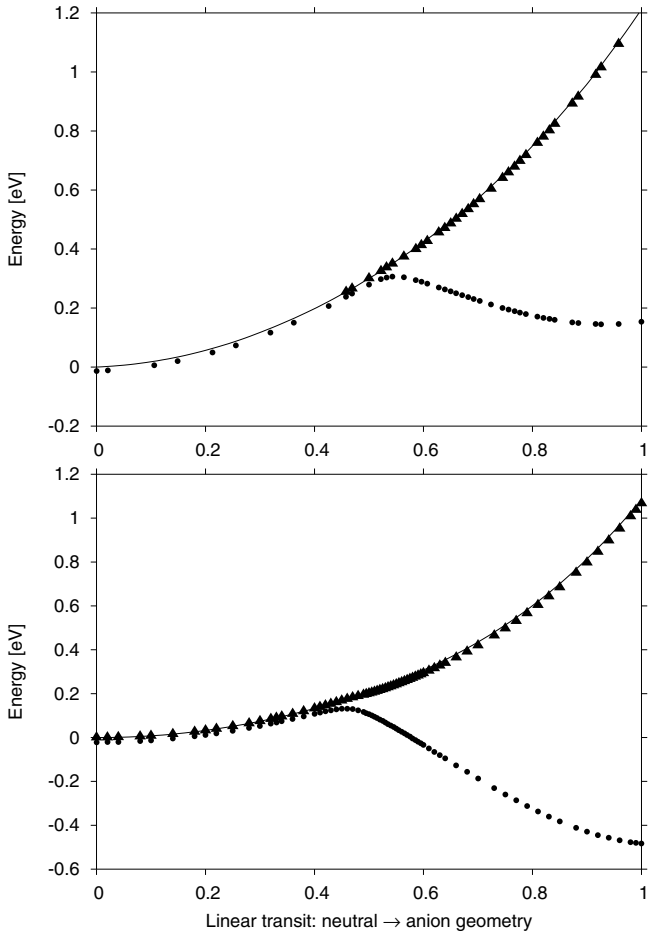

Fig. 2. One-dimensional cuts through the potential energy surfaces of neutral HC_3N and its anion. The cut is a linear transit form the equilibrium geometry of the neutral to that of the anion, where the equilibrium structures obtained at the CCSD(T)/AUG-cc-pVDZ level were used (cf. Fig. 1). In the upper panel the full line is the CCSD energy of the neutral, and the circles and triangles are the 1st and 2nd anionic states obtained at the EOM-CCSD level. In the lower panel the full line is the MP2 energy of the neutral, and the circles and triangles are the 1st and 2nd anionic states obtained at the ADC(2) level.

and restricted equilibrium geometries of neutral HCCCN and its valence anion. Note that the 'unrestricted' cut is analogous with the cuts used in references [14,15] serving as a reference; the 'restricted' cut is needed for the one-dimensional/two-dimensional comparison.

Ab initio results for the potential energy curves along the unrestricted cut obtained at the EOM-CCSD and ADC(2) levels of theory are shown in Figure 2. To facilitate comparison with references [14,15] we used CCSD and MP2 curves for the neutral, but we note that other choices are possible, and that it is not necessary to specify the neutral surface at all. The binding energies along the restricted cut look very similar, and we do not include an extra figure. Comparing the restricted and unrestricted ADC(2) curves the differences are less than 0.1 eV, and in case of the EOM-CCSD curves the difference is less than the symbol size in Figure 2. In conclusion, the geometrical restrictions imposed to obtain the restricted cut do shift the total energy, but have very little influence on the relative energies along the cuts.

To represent the one-dimensional curves the matrix elements of the model potential (Eq. (2)) were defined as follows

$$\begin{aligned} E_i(s) &= \epsilon_i + \kappa_i s + \gamma_i s^2 \qquad i = 1,2 \\ E_3 &= 0 \\ W_{1j} &= \text{const.} \qquad j = 2,3, \end{aligned} \tag{3}$$

where s is the coordinate along the cut with $s = 0$ referring to the structure of the neutral and $s = 1$ referring to the structure of the valence anion. We note that for symmetry reasons (see below) a linear ansatz for W_{1j} would be more appropriate, but, the coupling is small, and for fitting purposes only its value at the intersection matters (cf. [14,15]).

Fitting the 8 parameters ϵ_i, κ_i, γ_i, and W_{1j} to the four cuts (ADC(2)/EOM-CC restricted/unrestricted) we got in all cases χ^2 values in the order of a few μeV (the data sets comprised between 130 and 150 binding energies). Clearly, this functional form is extremely well suited to fit the ab initio EBEs along the cut. The value of the relevant coupling element W_{12} inferred from the unrestricted cut is 34 meV at the EOM-CCSD and 40 meV at the ADC(2) level, and the corresponding values extracted from the restricted cut are 32 and 30 meV. Thus, similar to the PES, at the ADC(2) level a somewhat greater sensitivity to restricting the geometrical parameters is found, but all in all the four values agree with each other remarkably well. Thus, based on the one-dimensional cuts connecting the equilibrium geometries of neutral and valence anion, we predict a coupling element of roughly 35 meV for the interaction of the dipole-bound and valence states of $HCCCN^-$. This value falls into the same order of magnitude as the couplings computed for nitromethane, uracil, and chlorouracil [14,15]. It is certainly a long shot to infer any general result from data for only four molecules, but for the time being a few ten meVs seem to be a good guess for the electronic coupling between a dipole-bound and a valence state.

Let us now turn to the two-dimensional cut. The origin of the coordinate system is again the geometry of the neutral, and the coordinates are ΔR and $\Delta\theta$, the changes in R and θ from their values in neutral HCCCN. The diabatic attachment energies $E_1(\Delta R, \Delta\theta)$ and $E_2(\Delta R, \Delta\theta)$ are Taylor-expanded around the geometry of the neutral, and including upto quadratic terms in ΔR and $\Delta\theta$ E_i reads

$$\begin{aligned} E_i = \epsilon_i + \kappa_R^{(i)}\Delta R + \kappa_\theta^{(i)}\Delta\theta + \gamma_{RR}^{(i)}\Delta R^2 \\ + \gamma_{R\theta}^{(i)}\Delta R\Delta\theta + \gamma_{\theta\theta}^{(i)}\Delta\theta^2 \quad i = 1,2, \end{aligned} \tag{4}$$

while keeping only linear terms one gets

$$E_i = \epsilon_i + \kappa_R^{(i)}\Delta R + \kappa_\theta^{(i)}\Delta\theta \qquad i = 1,2. \tag{5}$$

The off-diagonal coupling terms W_{1j} take in general the same form. Yet, for HCCCN in linear geometry ($\Delta\theta = 0$)

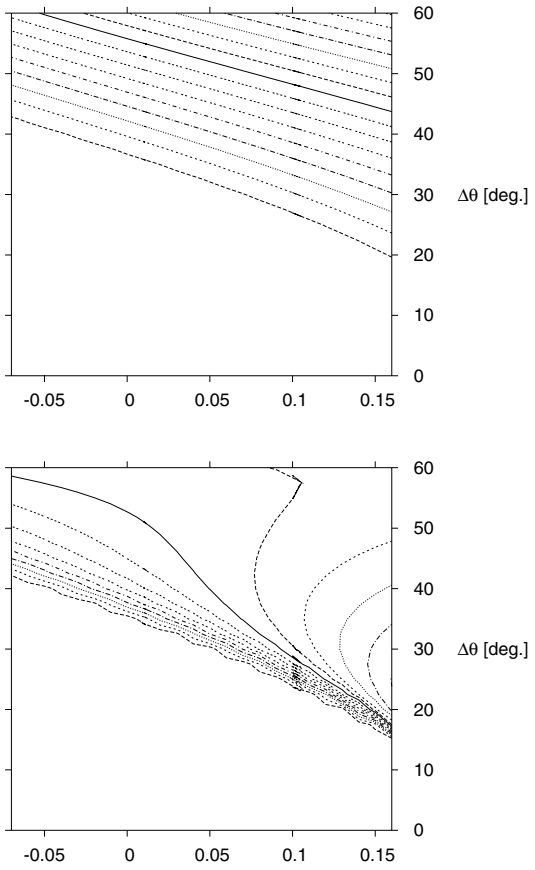

Fig. 3. Electron attachment energies of HC_3N computed at the EOM-CCSD level of theory. ΔR is the displacement of the CC triple bond and $\Delta\theta$ is the anti displacement of the HCC and the CCC angles. In the upper panel the attachment energy of the lower adiabatic state of the anion is displayed. The contour spacing is 0.1 eV, and, form the bottom, the first and last contours correspond to -0.1 and -1.6 eV, respectively. The large white area in the lower half of the plot corresponds to dipole-binding; the attachment energy in this region is about 10 meV. In the lower panel the second attachment energy is shown. The contours start at -1 meV, and the spacing is 1 meV. Here, in the white area the second attachment energy is positive, that is, the electron is not bound. Note the drastically different contour spacing in the panels.

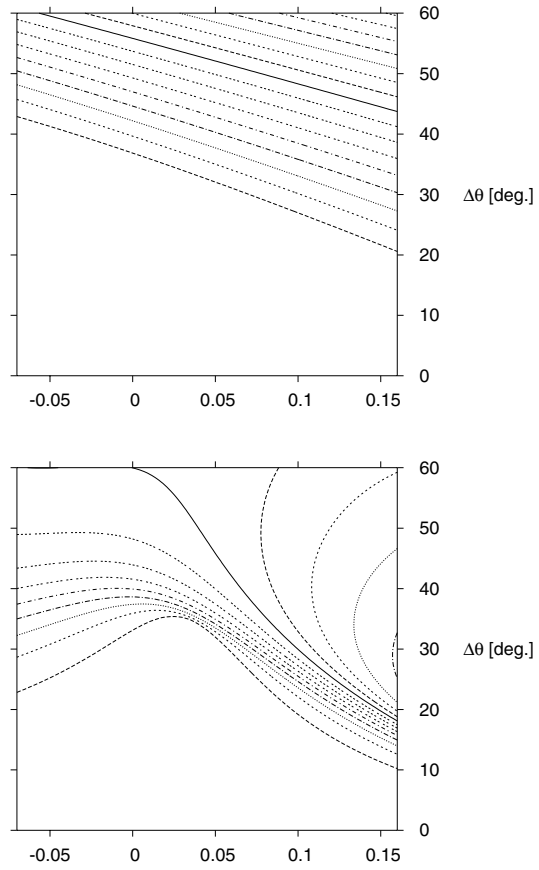

Fig. 4. Adiabatic attachment energies in the quadratic model. The parameters were fitted to the EOM-CCSD data shown in Figure 3, ΔR is the displacement of the CC triple bond, and $\Delta\theta$ is the anti displacement of the HCC and the CCC angles. In the upper panel the first attachment energy is displayed. From the bottom, contours start at -0.1 eV and decrease in 0.1 eV steps. The lower panel shows the second attachment energy; contours start at -1 meV and decrease in 1 meV steps.

the dipole-bound states have Σ symmetry whereas the valence state has Π symmetry, and consequently only terms odd in $\Delta\theta$ can couple these states. Including quadratic terms W_{1j} reads

$$W_{1j} = \lambda_\theta^{1j}\Delta\theta + 2\mu_{R\theta}^{1j}\Delta R\Delta\theta \qquad j = 2,3 \qquad (6)$$

while only the $\lambda_\theta^{1j}\Delta\theta$ term remains in linear approximation. Thus, in total there are 8 parameters in the linear and 16 parameters in the quadratic model. The ab initio data sets these parameters were fit to consisted of roughly 1200 (positive) EBEs, and the χ^2 values were in the 100 and 10 μeV range for the linear and quadratic models, respectively.

Contour plots of the adiabatic ab initio surfaces, the adiabatic surfaces as reproduced by the model potential, and the associated diabatic potentials are displayed in Figures 3, 4, and 5. The comparison of Figures 3 and 4 again shows, that the quadratic model represents the ab initio data astonishingly well. The diabatic potentials in Figure 5 are as expected smooth slowly varying functions, and provide — by construction — a mean to separately analyze the binding energies of the dipole-bound and the valence state. For small deviations from the geometry of the neutral, the EBE of the dipole-bound state is essentially a function of R in accordance with the expected variation of the dipole-moment with R and θ, and only for larger displacements of R the dipole-binding energy becomes a mild θ dependence. The variation of the valence binding energy is also very smooth and within the considered cut virtually

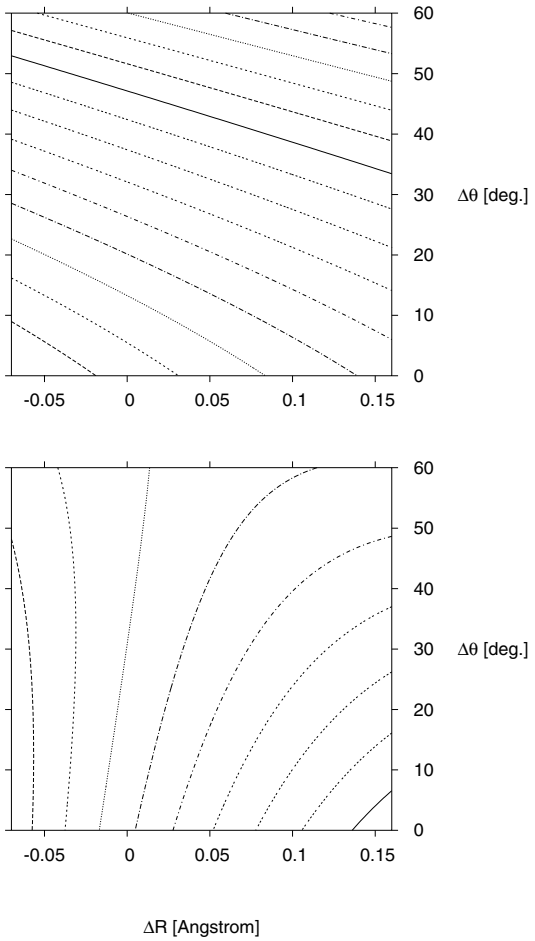

Fig. 5. Diabatic attachment energies in the quadratic model. The parameters were fitted to the EOM-CCSD data shown in Figure 3, ΔR is the displacement of the CC triple bond and $\Delta\theta$ is the anti displacement of the HCC and the CCC angles. In the upper panel the attachment energy corresponding to the valence state is displayed. From the lower left, contours start at +1.1 eV and decrease in 0.2 eV steps to -1.5 eV in the upper right. Positive attachment energies imply that the valence state is a resonance in this region. The lower panel shows the attachment energy of the diabatic dipole-bound state; contours start at −19 meV in the lower right and increase in 1 meV steps to −11 meV at the left edge.

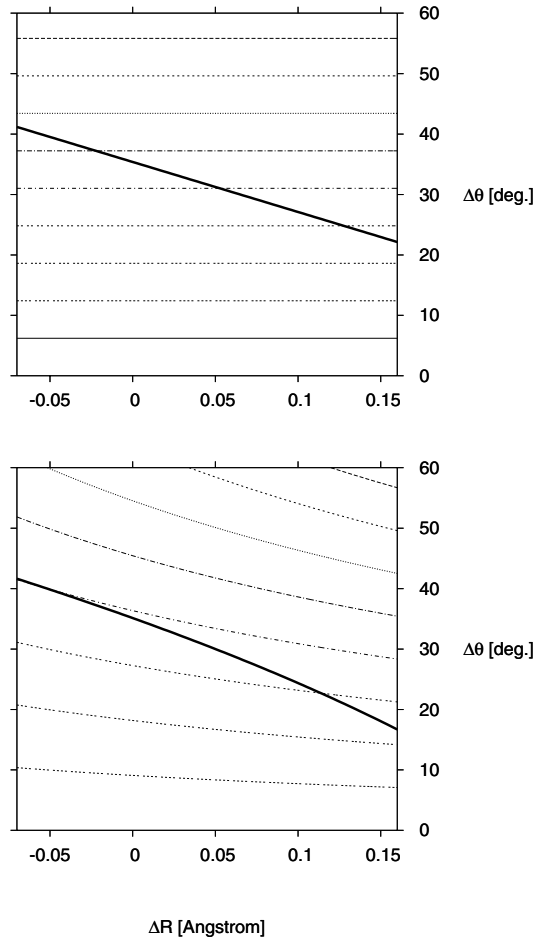

Fig. 6. Dipole-valence coupling matrix elements. The coupling elements of the linear and quadratic models are shown in the upper and lower panels, respectively. The results were obtained by fitting to the EOM-CCSD data shown in Figure 3. ΔR is the displacement of the CC triple bond and $\Delta\theta$ is the anti displacement of the HCC and the CCC angles. In both panels, the contours lines start at 10 meV from the bottom, and increase in 10 meV steps. The thick lines indicate the seams of intersection between the valence and dipole-bound states in the respective models.

a linear function of the nuclear coordinates. Clearly, only for appreciable bending angles, does the valence state represent a bound anion, whereas in the wide vicinity of the neutral geometry it represents a temporary anion with a negative binding energy.

Comparison at the ADC(2) level shows that at the geometry of the neutral, the diabatic (negative) binding energy of the valence state $E_1(\Delta R = 0, \Delta\theta = 0)$ is in excellent agreement with the real part of the Siegert energy obtained in the CAP/ADC(2) calculation. The agreement reflects essentially the conclusions of a recent investigation into the possibility of extrapolating bound state data into the metastable regime [39]. Extrapolation of an adiabatic surface can provide excellent approximations for resonance positions for unpolar molecules, and the authors of reference [39] were careful to point out that this technique is in principle unsuitable for polar molecules, since here a valence state will turn adiabatically into a dipole-bound species making the adiabatic energy unsuitable for extrapolation. Yet, the diabatic model potential does provide a mean for using an extrapolation method *in the presence of a dipole-bound state*, that is, a mean for obtaining the real part of the potential energy surface of temporary anions. Comparison for HCCCN at the ADC(2) level shows that the extrapolation works, and using the model parameters fitted to the EOM-CCSD results, we find a resonance position of 1.0 eV for the lowest $^2\Pi$ state of HCCCN, only slightly higher than the ADC(2) value.

The coupling element between the two diabatic states is shown in Figure 6. Comparison of the upper and lower panels shows that the linear model accounts for all

qualitative features of the coupling. Thus, a linear model may be a worthwhile alternative in higher dimensions when the number of available ab initio points per degree of freedom becomes small and the number of parameters in the quadratic model becomes large. In contrast to the one-dimensional cut, within the two-dimensional model we are now in a position to analyze the variation of the coupling element with the nuclear coordinates. The electronic coupling is most relevant close to the intersection seam of the two diabatic state which has been indicated as a thick line in Figure 6. In the region of the seam, W_{12} shows values between 20 and 40 meV (upto 50 meV in the linear model; Fig. 6). This is a pronounced yet not dramatic dependency. We conclude that for any quantitative treatment the variation of the coupling needs to be taken into account, and a multidimensional description of the dynamics is required. However, for qualitative considerations a typical value can be sufficient, and, at least for HCCCN, any reasonably chosen one-dimensional cut will indeed provide that.

5 Conclusions

Using high level ab initio methods we have studied the electron acceptor properties of HCCCN focusing in particular on the coupling between its dipole-bound and its valence anion. Regarding the key energetic properties, we predict an EA of 9 meV associated with the dipole-bound state. At the geometry of neutral HCCCN the valence anion is a short-lived temporary π^* state, and we predict a resonance position of 0.7 eV and a resonance width of 0.15 eV (lifetime of 4 fs). Yet, by folding into a zig-zag chain the valence anion becomes electronically stable, and at the anion's equilibrium geometry we predict a VDE of 1.25 eV. These three predictions can directly be tested in Rydberg electron transfer, electron transmission, and photo detachment experiments, respectively. Regarding the adiabatic EA our results show that neutral HCCCN and its valence anion are almost isoenergetic. At the highest theoretical level employed we find an small positive adiabatic EA of 50 meV that is dominated by the zero-point correction. This value is smaller than the anticipated accuracy of our calculations, but we are confident to predict a small positive adiabatic EA. In particular, we can conclude that the adiabatic EA found in the NIST webbook is not that of HCCCN, but that of a different C_3HN molecule.

The electronic coupling of the dipole-bound and the valence state has been addressed in the framework of a diabatic model potential. As the potential energy surfaces the coupling between them is a function of the nuclear coordinates, and a two-dimensional cut through the PES of $HCCCN^-$ — as suggested by the geometrical change between neutral HCCCN and its valence anion — allowed us for the first time to study this dependency. In the region of the intersection seam between the diabatic dipole-bound and valence state, where the coupling exerts its strongest influence, its value changes strongly, yet, it stays in the order of magnitude of a few ten meV. Thus, for any quantitative consideration one needs to include the variation of the coupling, and our diabatic model potential provides the means for studying the detailed dynamics of the intramolecular electron transfer in HCCCN. On the other hand, for more qualitative considerations, such as analyzing trends between different molecules, a typical value of the coupling will suffice, and comparison with one-dimensional cuts shows that it is possible to extract a typical value from any reasonably chosen one-dimensional cut.

A typical value for the electronic coupling in HCCCN is 35 meV, a value in the same order of magnitude as those predicted for nitromethane and uracil [14,15]. We conclude that the intramolecular electron transfer from the molecular periphery onto the nuclear framework is still in the diabatic but close to the adiabatic regime. Thus, while it is true that dipole-bound electrons reside in very diffuse orbitals well outside the van-der-Waals surface of the neutral, and their influence on the geometry of the nuclear framework is often negligible, dipole-bound electrons can — via the coupling to valence states — exert a strong influence in the inner molecular region and represent efficient 'doorways' [6] for vibrational excitation or chemical reactions.

Finally let us briefly mention that the diabatic model potential, which has here been used to extract the coupling from the adiabatic ab initio data, does provide a mean for extrapolating the valence state surface into the metastable regime. Whereas extrapolation of adiabatic surfaces will only yield meaningful results for unpolar molecules [39], the model potential will even work in the presence of dipole-bound states, since their existence is properly taken into accounts — always provided that enough bound state data for both anionic states are available for a stable fit. For HCCCN the energy of the diabatic valence state virtually reproduces the resonance position from our CAP/ADC(2) calculations.

All in all, HCCCN is a very interesting and theoretically challenging system, since its dipole-bound and valence states are almost isoenergetic. Thus, there is a very good chance to observe both states and the associated electron transfer dynamics in an experiment. We hope our work will stimulate experimental studies on this prototypical system.

We gratefully acknowledge stimulating discussions with L.S. Cederbaum, H.-D. Meyer, and K.D. Jordan.

References

1. *CRC Handbook of Chemsitry and Physics*, edited by D.R. Lide, 79th edn. (CRC Press, Boca Raton, 1998)
2. K.D. Jordan, F. Wang, Annu. Rev. Phys. Chem. **54**, 367 (2003)
3. R.N. Compton, N.I. Hammer, *Advances in Gas-Phase Ion Chemistry*, edited by N.G. Adams, L.M. Babcock, (JAI Press, Stamford, Connecticut, 2001), Vol. 4, pp. 257–305
4. C. Desfrançois, H. Abdoul-Carime, J.-P. Schermann, Int. J. Mol. Phys. B **10**, 1339 (1996)

5. *Theoretical prospect of negative ions*, edited by J. Kalcher (Research Signpost, Kerala, India, 2002)
6. R.N. Compton, H.S. Carman Jr, C. Defrançois, H. Abdoul-Carmine, J.P. Schermann, J.H. Hendricks, S.A. Lyapustina, K.H. Bowen, J. Chem. Phys. **105**, 3472 (1996)
7. C. Desfrançois, V. Periquet, S.A. Lyapustina, T.P. Lippa, D.W. Robinson, K.H. Bown, H. Nonaka, R.N. Compton, J. Chem. Phys. **111**, 4569 (1999)
8. E. Leber, S. Barsotti, I.I. Fabrikant, J.M. Weber, M.-W. Ruf, H. Hotop, Eur. Phys. J. D **12**, 125 (2000)
9. J.M. Weber, W.H. Robertson, M.A. Johnson, J. Chem. Phys. **115**, 10718 (2001)
10. H. Hotop, M.-W. Ruf, M. Allan, I.I. Fabrikant, Adv. At. Mol. Opt. Phys. **49**, 85 (2003)
11. A. Schramm, I.I. Fabrikant, J.M. Weber, E. Leber, M.-W. Ruf, H. Hotop, J. Phys. B **32**, 2153 (1999)
12. M. Stepanović, Y. Pariat, M. Allan, J. Chem. Phys. **110**, 11376 (1999)
13. A.M. Scheer, K. Aflatooni, G.A. Gallup, P.D. Burrow, Phys. Rev. Lett. **92**, 068102 (2004)
14. T. Sommerfeld, Phys. Chem. Chem. Phys. **4**, 2511 (2002)
15. T. Sommerfeld, J. Phys. Chem. A **108**, 9150 (2004)
16. T. Sommerfeld, J. Phys. Conf. Ser. **4**, 245 (2005)
17. W. von Niessen, J. Schirmer, L.S. Cederbaum, Comp. Phys. Rep. **1**, 57 (1984)
18. J.V. Ortiz, V.G. Zakrzewski, O. Dolgounitcheva, *Conceptual trends in Quantum Chemistry*, edited by E. Kryachko (Kluwer, Dordrecht, 1997)
19. J. Schirmer, L.S. Cederbaum, O. Walter, Phys. Rev. A **28**, 1237 (1983)
20. M. Nooijen, R.J. Bartlett, J. Chem. Phys. **102**, 3629 (1995)
21. F. Mertins, J. Schirmer, Phys. Rev. A **53**, 2140 (1996)
22. F. Mertins, J. Schirmer, Phys. Rev. A **53**, 2153 (1996)
23. G. Jolicard, E.J. Austin, Chem. Phys. Lett. **121**, 106 (1985)
24. U.V. Riss, H.-D. Meyer, J. Phys. B **26**, 4503 (1993)
25. T. Sommerfeld, U.V. Riss, H.-D. Meyer, L.S. Cederbaum, B. Engels, H.U. Suter, J. Phys. B **31**, 4107 (1998)
26. S. Feuerbacher, T. Sommerfeld, R. Santra, L.S. Cederbaum, J. Chem. Phys. **118**, 6188 (2003)
27. R.A. Kendall, T.H. Dunning Jr, R.J. Harrison, J. Chem. Phys. **96**, 6769 (1992)
28. T.H. Dunning Jr, J. Chem. Phys. **55**, 716 (1971)
29. Computer code ACES II, Quantum Theory Project, University of Florida (1998)
30. Computer code Molcas Version 5, University of Lund, Sweden (2001)
31. D.C. Clary, J. Phys. Chem. **92**, 3173 (1988)
32. M. Gutowski, P. Skurski, A.I. Boldyrev, J. Simons, K.D. Jordan, Phys. Rev. A **54**, 1906 (1996)
33. G.L. Gutsev, M. Nooijen, R.J. Bartlett, Chem. Phys. Lett. **276**, 13 (1997)
34. P. Skurski, , M. Gutowski, J. Simons, Int. J. Quant. Chem. **80**, 1024 (2000)
35. L.A. Curtiss, P.C. Redfern, K. Raghavachari, V. Rassolov, J.A. Pople, J. Chem. Phys. **110**, 4703 (1999)
36. M. Heni, E. Illenberger, Int. J. Mass Spectrom. **73**, 127 (1986)
37. T.F. O'Malley, Adv. At. Mol. Phys. **7**, 223 (1971)
38. T. Pacher, L.S. Cederbaum, H. Köppel, Adv. Chem. Phys. **84**, 293 (1993)
39. S. Feuerbacher, T. Sommerfeld, L.S. Cederbaum, J. Chem. Phys. **121**, 6628 (2004)